Optimal Operation Strategy for Multi-Energy Microgrid Participating in Auxiliary Service

Yahui Wang, Yong Li, *Senior Member, IEEE*, Yijia Cao, *Senior Member, IEEE*, Mohammad Shahidehpour, *Life Fellow, IEEE*, Lin Jiang, *Member, IEEE*, Yilin Long, Youyue Deng, Weiwei Li

***Abstract*—Since multi-energy microgrid (MEMG) can coordinate various resources to operate as a virtual power plant (VPP), it is an important way to maintain the stable and economic operation of the power systems and decrease the impact of intermittence of distributed energy resources (DERs). However, the potential of MEMG as a VPP has not been thoroughly explored since auxiliary service (AS) market is not fully open for MEMG at present. The relevant challenges include balancing conflict of interests among multiple energy entities, motivating users to adjust flexible loads, integrating multiple flexible resources in energy supply/demand sides and formulating specific policies, etc. To handle these tasks, an optimal operation strategy for MEMG participating in AS is proposed by considering Stackelberg game theory and integrated demand response (IDR). The feasibility of the proposed strategy is validated by a practical MEMG in Hunan, China. The results show that the economic benefits of energy entities are effectively raised and the peak-shaving AS is realized while user satisfaction is also maintained. This work would give reference to the constructor of future AS market to formulate polices about the operation modes and pricing schemes of MEMG.**

***Index Terms*—Auxiliary service, integrated demand response, multi-energy microgrid, peak shaving.**

NOMENCLATURE

Abbreviations:

AS	Auxiliary service
DERs	Distributed energy resources
DSM	Demand side management
ESS	Energy storage system
IDR	Integrated demand response
KKT	Karush-Kuhn-Tucker
LBU	Lithium bromide unit
MEMG	Multi-energy microgrid

Parameters:

BC_{o}	Cost of buying electricity and gas for operator
c_{cf}	Cooling coefficient of centrifuge
c_{h}	Heating coefficient of heaters
$c_{\mathrm{li,h/c}}$	Heating/cooling coefficient of LBU
$C_{\mathrm{cf,min/max}}$	Minimum/maximum cooling power of centrifuge
$CC_{\mathrm{ct},i}$	Cooling energy cost of $\mathrm{User}_{\mathrm{ct},i}$
CI_{o}	Cooling energy income of operator
d_{w}	Density of water
$EC_{\mathrm{e},j}$	Electricity cost of $\mathrm{User}_{\mathrm{e},j}$
EC_{cur}	Electricity cost of $\mathrm{User}_{\mathrm{e}}$ in current mode
$E_{\mathrm{ct},i/\mathrm{e},j/\mathrm{o}}$	Compensation of $\mathrm{User}_{\mathrm{ct},i}$/$\mathrm{User}_{\mathrm{e},j}$/operator
$F_{\mathrm{ct},i/\mathrm{e},j/\mathrm{o}}$	Objective function of $\mathrm{User}_{\mathrm{ct},i}$/$\mathrm{User}_{\mathrm{e},j}$/operator
$HC_{\mathrm{ct},i}$	Thermal energy cost of $\mathrm{User}_{\mathrm{ct},i}$
$H_{\mathrm{h,min/max}}$	Minimum/maximum thermal power of heaters
HI_{o}	Thermal energy income of operator
$p_{\mathrm{b,lo/up}}$	Lower/upper limit of average compensation price
$p_{\mathrm{b,min/max}}$	Minimum/maximum value of compensation price
$p_{\mathrm{e,av}}$	Upper limit of the average electricity price
$p_{\mathrm{e,min/max}}$	Minimum/maximum electricity price
ΔP_{av}	Average load change compared to benchmark
P_{av}	Average load power of benchmark case
$P_{\mathrm{ess,max}}$	Maximum charging/discharging power of ESS
$P_{\mathrm{ge,min/max}}$	Minimum/maximum power of gas turbine
$P_{\mathrm{li,min/max}}$	Minimum/maximum power of LBU
$P_{\mathrm{tld,min/max}}$	Minimum/maximum transferable load
$P_{\mathrm{rld,max}}$	Maximum reduced electrical load
$Q_{\mathrm{min},i}$	Minimum cooling/thermal load of $\mathrm{User}_{\mathrm{ct},i}$
$Q_{\mathrm{max},i}$	Maximum cooling/thermal load of $\mathrm{User}_{\mathrm{ct},i}$
$S_{\mathrm{ess,min/max}}$	Minimum/maximum storage capacity of ESS
$T_{\mathrm{s/e}}$	Start/end time of AS period
$T_{\mathrm{em,min/max}}$	Minimum/maximum temperature of water
$\mathrm{User}_{\mathrm{ct}}$	Users that consume cooling and thermal energy
$\mathrm{User}_{\mathrm{ct},i}$	The i^{th} user in the set of $\mathrm{User}_{\mathrm{ct}}$
$\mathrm{User}_{\mathrm{e}}$	Users that consume electricity
$\mathrm{User}_{\mathrm{e},j}$	The j^{th} user in the set of $\mathrm{User}_{\mathrm{e}}$
USI	User satisfaction index
∂_{w}	Specific heat capacity of water
μ	Reduction coefficient of electricity cost of $\mathrm{User}_{\mathrm{e}}$
$\eta_{\mathrm{ch/dis}}$	Charging/discharging efficiency of ESS
$\eta_{\mathrm{ge,e}}$	Electricity efficiency of gas turbine
$\eta_{\mathrm{ge,h}}$	Thermal energy efficiency of gas turbine

This work was supported in part by the International Science and Technology Cooperation Program of China under grant 2022YFE0129300, in part by the National Natural Science Foundation of China under Grant U22B200134, in part by the Royal Society-Newton Advanced Fellowship under grant NAF\R1\201036, and in part by the 111 Project of China under Grant B17016. (Corresponding author: Y. Li and Y. Cao)

Y. Wang, Y. Li, Y. Cao and Y. Deng are with the College of Electrical and Information Engineering, Hunan University, Changsha 410082, China. (e-mail: wangyh1993@hnu.edu.cn, yongli@hnu.edu.cn, yjcaohnu@163.com, dengyouyue@hnu.edu.cn).

M. Shahidehpour is with the Galvin Center for Electricity Innovation, Illinois Institute of Technology, Chicago, IL 60616, USA. (e-mail: ms@iit.edu).

L. Jiang is with the Department of Electrical Engineering and Electronics, University of Liverpool, Liverpool L693BX, U.K. (e-mail: l.jiang@liverpool.ac.uk)

Y. Long is with the State Grid Hunan Power Supply Service Center (Metrology Center), Changsha 410116, China. (e-mail: longyilin@hnu.edu.cn)

W. Li is with the Integrated Energy Division of ENN Gas Co., Ltd, Changsha 410000, China. (e-mail: 279017601@qq.com)

λ_{gas}	Calorific value of natural gas
γ	loss rate of ESS
Indices:	
i/*j*	Index of User_{ct}/User_{e}, from 1 to *m*/*n*
k/*r*	Number of inequality/equality constraint
t	Index of time, from 0 to T
Variables:	
$C_{\text{cf/li}}(t)$	Output cooling power of centrifuge/LBU at *t*
$f_k(t)$	The k^{th} inequality constraints at *t*
$H_{\text{ge}}(t)$	Waste thermal power of gas turbine at *t*
$g_r(t)$	The r^{th} equality constraints at *t*
$H_{\text{li/h}}(t)$	Output thermal power of LBU/ heaters at *t*
$L_r(t)$	Lagrange multiplier for r^{th} equality constraint
$M_k(t)$	Lagrange multiplier for k^{th} inequality constraint
$p_{\text{b/be}}(t)$	Compensation price for flexible loads/electricity
$p_{\text{bo}}(t)$	Compensation price for operator at *t*
$p_{\text{buy}}(t)$	Price for buying electricity from the power grid
$p_{c/h/e}(t)$	Price for cooling/thermal/electrical energy at *t*
$p_{\text{n}}(t)$	Price for purchasing natural gas at *t*
$p_{\text{pur}}(t)$	Price for purchasing thermal and cooling energy
$P(t)$	Load power at *t* of benchmark case
$P_{\text{grid}}(t)$	Electrical power from the power grid at *t*
$P_{\text{ch/dis}}(t)$	Charging/discharging power at *t*
$P_{\text{cf}}(t)$	Electricity consumption of centrifuge at *t*
$P_{\text{cur},j}(t)$	Power consumption of $\text{User}_{\text{e},j}$ in current mode
$P_{\text{e},j}(t)$	Electricity consumption of $\text{User}_{\text{e},j}$ at *t*
$P_{\text{ge}}(t)$	Output electricity of gas turbine at *t*
$\Delta P(t)$	Power change at *t* compared to benchmark case
$\Delta P_0(t)$	Power participated in AS of operator at *t*
$\Delta P_{\text{tld},j}(t)$	Load transferred of $\text{User}_{\text{e},j}$ at *t*
$\Delta P_{\text{rld},j}(t)$	Load reduced of $\text{User}_{\text{e},j}$ at *t*
$Q_{\text{c},i}(t)$	Cooling power consumption of $\text{User}_{\text{ct},i}$ at *t*
$Q_{\text{ct},i}(t)$	Thermal/cooling load of $\text{User}_{\text{ct},i}$
$Q_{\text{h},i}(t)$	Thermal power consumption of $\text{User}_{\text{ct},i}$ at *t*
$Q_{\text{cur},i}(t)$	Energy consumption of $\text{User}_{\text{ct},i}$ in current mode
$Q_{\text{aux},i}(t)$	Energy consumption of $\text{User}_{\text{ct},i}$ when joining AS
$\Delta Q_{\text{ct},i}(t)$	Reduced cooling/thermal power of $\text{User}_{\text{ct},i}$ at *t*
$s_{\text{ch/dis}}(t)$	Charging/discharging state of ESS at *t*
$s_{\text{li,h/c}}(t)$	Heating/cooling state of LBU at *t*
$S_{\text{ess}}(t)$	Storage capacity of ESS at *t*
$T_{\text{em,in}}(t)$	Initial temperature of water at *t*
$V_{\text{gas}}(t)$	Volume of natural gas purchased from gas station
$V_{\text{ge/h}}(t)$	Volume of gas consumed by gas turbine/heaters
$V_{\text{w},i}(t)$	Volume of water supplied to $\text{User}_{\text{ct},i}$ at *t*

I. Introduction

Multi-energy microgrid (MEMG), featured by diverse forms of energy such as cooling, thermal, electrical energy, is a bond between multiple energy resources/loads and the power grid. In other words, it can act as a virtual power plant (VPP) by integrating diverse types of distributed energy resources (DERs) and various flexible loads to provide energy support to the power grid. Clearly, MEMG has the potential to decrease the impact of intermittence of DERs and maintain the stable and economic operation of the power systems. As a result, the studies on how to exploit this potential of MEMG is receiving increasing attentions worldwide.

Currently, there are many works carried out on the optimal operation strategies of microgrid [1], [2], which are foundations for that of MEMG[3]. The operation targets of microgrid include improving economy [4], achieving energy self-sufficiency [5], reducing harmful emission and meeting user preferences [6], etc. To achieve these goals, many works are conducted: (1) demand side management (DSM) [7] is studied to explore the potential of flexible loads in reducing the difference between power valley and peak; (2) DERs are aggregated to form an energy hub or a VPP [8], [9] to supply reliable energy to the power systems; and (3) flexible resources of both supply and demand sides in microgrid are integrated to participate in auxiliary service (AS) [3]. However, the operation strategies of microgrid cannot be applied directly to MEMG, since microgrid only involves electricity in most conditions, while MEMG contains diverse forms of energy and multiple energy entities. Therefore, the operation strategies of MEMG are much more complex than that of microgrid.

The challenges of optimizing the operation of MEMG, include: (1) balancing conflict of interests among multiple energy entities, (2) motivating diverse users to adjust flexible loads and (3) integrating multiple flexible resources in energy supply and demand sides, etc. To handle the first issue, game theory is a solution. It can be classified into two types: cooperative game theory and non-cooperative one [10]. The former is always applied to form an alliance among different entities to rationally allocate profits [11], and the latter is used to handle the conflicting interests in competitions among multiple entities [12]. Although many literatures adopt game theory to the cases such as energy trading [13],[14], cost optimization [15] and energy management [16], [17], there are few works use it for the game among different energy entities in MEMG. Facing the second and third challenges, approaches such as integrated demand response (IDR) [18]–[20], multi-energy hub or VPP [21] are proposed.

Although there are several literatures addressing one or two of the above challenges of MEMG, most of them lack validation of practical engineering cases. The reason lies in the fact that the number of practical engineering applications of MEMG is limited, and the parameters and operating data of them are always confidential. Another current bottleneck for the researches on optimal operation of MEMG is that the energy market is not fully open for MEMG. In China, MEMG is not allowed to send back surplus energy to the power grid, let alone involve in the AS. Therefore, there is a need for investigating the involvement of MEMG in AS market.

However, it is an inevitable trend for MEMG participating in AS in the future when relevant technologies are mature and related polices are established. Both users in MEMG and the power systems would benefit from it. On the one hand, users are provided with comprehensive energy services and economic compensation. On the other hand, the impact of the randomness of DERs is decreased by energy aggregation, which is conducive to the safe and reliable operation of the power grid. Obviously, it is a potential win-win operation mode of MEMG, which is worthy of further explorations.

In response to the above challenges and motivations, an optimal operation strategy for MEMG participating in AS is proposed in this paper based on a practical application of MEMG in Hunan, China. Specifically, the highlights of this work include: (1) a two-layer game model is built to coordinate the conflicting interests among multiple energy entities in MEMG via price adjustments; (2) multiple forms of flexible energy in MEMG are motivated and integrated to join AS market; and (3) four comparative cases are set up based on the practical MEMG project to validate the feasibility of the proposed operation strategy.

The rest of the paper is organized as follows. In Section II, the schematic of a typical MEMG is introduced, and a practical MEMG in China is given as an example to discuss the potential operation mode to participate in AS market. The principals and models of the proposed operation strategy are presented in Section III. In Section IV, validation and analysis are carried out. Finally, Section V concludes the paper.

II. Structure and Operation of MEMG

A. Structure of MEMG

In MEMG, the most common energy forms are electricity, cooling energy and thermal energy. The schematic of a typical MEMG is shown in Fig. 1, which consists of devices for energy generation, storage, transformation and consumption of diverse forms of energy.

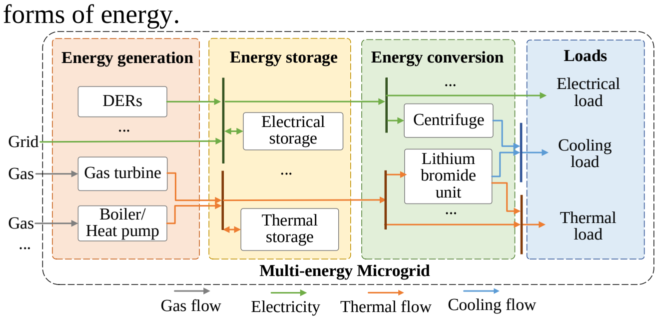

Fig. 1 The schematic of a typical MEMG.

Fig. 2 The panorama of the practical MEMG in Hunan, China.

Fig. 2 presents the panorama of a practical engineering demonstration of MEMG that located in Hunan, China, which is positioned as a world advanced level tourism resort and conference center. Currently, it includes a multi-energy station and plenty of energy users in recreation area and living area (e.g., hotels), with a designed total energy supply area of 357,000 m^2. The structure of the practical MEMG project is displayed Fig. 3, in which the multi-energy station acts as the heart of it. It supplies electrical, cooling and thermal energy to users to meet their different energy preferences: users in recreation area only consume cooling and thermal energy from the station; users in living area consume electricity from the station if the station has surplus electrical power, otherwise they purchase electricity from the power grid. To simplify the expression, the former type of users is denoted as $\mathrm{User_{ct}}$ ($\mathrm{User_{ct}}$ ={$\mathrm{User_{ct,1}}$,…, $\mathrm{User}_{\mathrm{ct},i}$, $\mathrm{User}_{\mathrm{ct},m}$ }) and the latter is represented as $\mathrm{User_e}$ ($\mathrm{User_e}$={$\mathrm{User_{e,1}}$,…, $\mathrm{User}_{\mathrm{e},j}$, $\mathrm{User}_{\mathrm{e},n}$}).

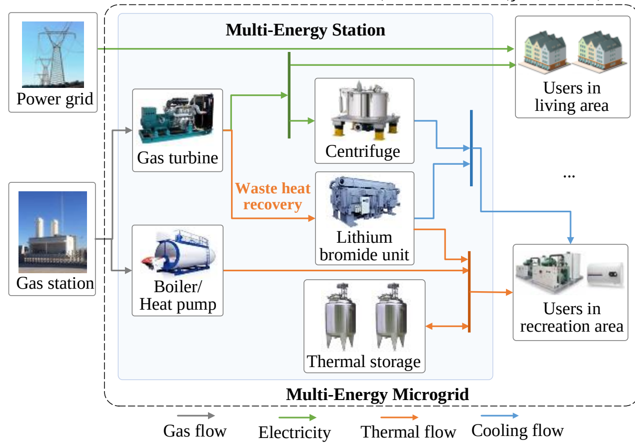

Fig. 3 The structure of the practical MEMG in Hunan, China.

B. Operation Modes

1) Current operation mode

MEMG is not allowed to send surplus energy back to the power grid at present, and the current operation mode of the practical MEMG is shown in Fig. 4, i.e., the multi-energy station supplies $\mathrm{User_{ct}}$ with thermal and cooling energy, and $\mathrm{User_e}$ buy electricity from the power grid if the surplus electricity from the multi-energy station is insufficient. Although in the current operation mode, multi-energy station can gain economic benefit by supplying energy to users and users can get a variety of energy supplies, this operation mode still has limitations: (1) the cost for $\mathrm{User_e}$ purchasing electricity from the power grid is high; (2) the potential of MEMG to supply power to the power grid is ignored; and (3) the potential of flexible loads to reduce power fluctuation is not explored.

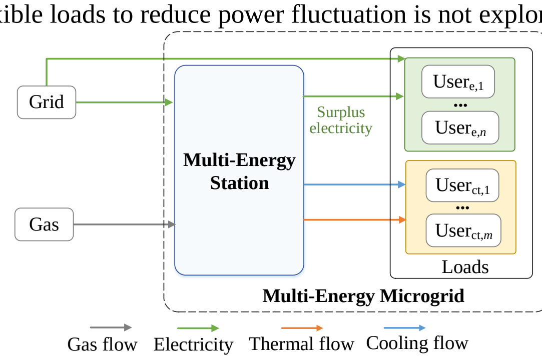

Fig. 4 Current operation mode of the MEMG.

2) Potential operation mode

To address the above limitations and provide a forward-looking suggestion for the MEMG when AS market is open in the future, a potential operation mode for MEMG participating in AS is designed in Fig. 5. First, the multi-energy station (i.e., operator of the MEMG) receives the signal of AS from the power grid. After that, it delivers the compensation incentive and AS requirement to users, and users adjust flexible loads accordingly. Then, operator integrates flexible resources and feeds energy back to join in AS.

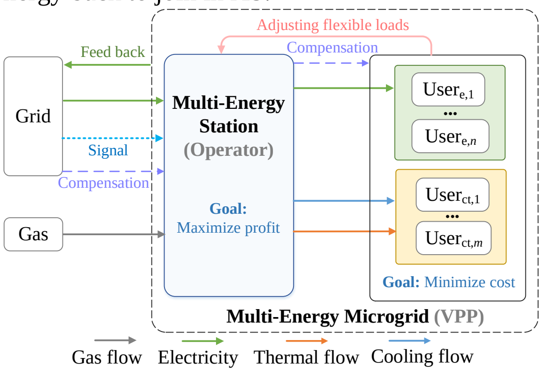

Fig. 5 Potential operation mode of MEMG.

In the potential mode, (1) User$_{e}$ can buy electricity from the multi-energy station with lower agreement price than that when trading with the power grid, and both the multi-energy station and users will benefit; (2) multi-energy station acts as operator to integrate energy resources in MEMG to supply power to the power grid; and (3) both the multi-energy station and users obtain economic compensation by adjusting flexible resources, and the peak-shaving AS is realized. The comparison of the two modes is shown in Table I.

TABLE I
COMPARISON OF CURRENT MODE AND POTENTIAL MODE

Limitations of current mode	Advantages of potential mode
• High price for User$_{e}$ when buying electricity from power grid	• Lower agreement price for User$_{e}$ when trading with multi-energy station
• There is no operator to integrate and flexible resources, e.g., DERs	• Multi-energy station acts as an operator to integrate flexible resources
• Users cannot gain economic benefit in this mode	• Users gain economic compensation by adjusting flexible loads
• Flexible loads are not utilized	• IDR is realized
• MEMG cannot send power back to the power grid	• MEMG can participate in AS

Notably, the potential operation mode is designed based on these assumptions: (1) an agreement on electricity price is made between the multi-energy station and User$_{e}$ to benefit both sides; (2) multi-energy station becomes the operator of the MEMG; (4) MEMG is allowed to send surplus energy back to the power grid; and (5) AS market is open for MEMG.

III. OPTIMAL OPERATION STRATEGY

To realize the designed operation mode of the MEMG, an operation strategy is proposed. The mathematical modelling of users and operator, game balancing among different energy entities and optimization problem solving are given.

A. Modelling of Energy Entities

1) Model of User$_{ct}$

The objective function $F_{\mathrm{ct},i}$ of User$_{\mathrm{ct},i}$ is composed of the cost for energy consumption and the economic compensation for participating in AS, as expressed in Eq.(1).

$$F_{\mathrm{ct},i}=\min(HC_{\mathrm{ct},i}+CC_{\mathrm{ct},i}-E_{\mathrm{ct},i}) \tag{1}$$

where $F_{\mathrm{ct},i}$ denotes the operation cost of User$_{\mathrm{ct},i}$ for a period of time (e.g., a day), $HC_{\mathrm{ct},i}$ is the cost for thermal energy, $CC_{\mathrm{ct},i}$ is the cost for cooling energy, and $E_{\mathrm{ct},i}$ is the economic compensation.

$$HC_{\mathrm{ct},i}=\sum\nolimits_{t=1}^{T}Q_{\mathrm{h},i}(t)\cdot p_{\mathrm{h}}(t) \tag{2}$$

$$CC_{\mathrm{ct},i}=\sum\nolimits_{t=1}^{T}Q_{\mathrm{c},i}(t)\cdot p_{\mathrm{c}}(t) \tag{3}$$

$$E_{\mathrm{ct},i}=\sum\nolimits_{t=T_{\mathrm{s}}}^{T_{\mathrm{e}}}[\sum\Delta Q_{\mathrm{ct},i}(t)\cdot p_{\mathrm{b}}(t)] \tag{4}$$

$$\Delta Q_{\mathrm{ct},i}(t)=Q_{\mathrm{cur},i}(t)-Q_{\mathrm{aux},i}(t) \tag{5}$$

The expressions for $HC_{\mathrm{ct},i}$, $CC_{\mathrm{ct},i}$ and $E_{\mathrm{ct},i}$ are shown in Eqs.(2)-(5), respectively. t denotes the moment, which is from 1 to T.$Q_{\mathrm{h},i}(t)$ is the thermal power consumption of User$_{\mathrm{ct},i}$ at t. $p_{\mathrm{h}}(t)$ is the thermal energy price at t. $Q_{\mathrm{c},i}(t)$ is the cooling power consumption at t. $p_{\mathrm{c}}(t)$ is the cooling energy price at t. $[T_{\mathrm{s}},T_{\mathrm{e}}]$ is the AS period. $\Delta Q_{\mathrm{ct},i}(t)$ refers to the reduced cooling and thermal power at t, which is calculated by the energy consumption $Q_{\mathrm{cur},i}(t)$ in current operation mode subtracting the energy consumption $Q_{\mathrm{aux},i}(t)$ when joining AS. $p_{\mathrm{b}}(t)$ refers to compensation prices of flexible cooling/thermal loads.

The cooling/thermal energy is supplied by providing cold or hot water to users through the pumps. There is an acceptable range of water temperature of users, hence the flexible cooling/thermal load $Q_{\mathrm{ct},i}(t)$ is obtained by Eq.(6).

$$Q_{\min,i}\le Q_{\mathrm{ct},i}(t)\le Q_{\max,i} \tag{6}$$

$$Q_{\min,i}=\partial_{\mathrm{w}}\cdot d_{\mathrm{w}}\cdot V_{\mathrm{w},i}(t)\cdot(T_{\mathrm{em,in}}(t)-T_{\mathrm{em,min}}) \tag{7}$$

$$Q_{\max,i}=\partial_{\mathrm{w}}\cdot d_{\mathrm{w}}\cdot V_{\mathrm{w},i}(t)\cdot(T_{\mathrm{em,max}}-T_{\mathrm{em,in}}(t)) \tag{8}$$

where $Q_{\min,i}$ and $Q_{\max,i}$ represent the minimum and maximum cooling/thermal load, respectively. ∂_{w} denotes the specific heat capacity of water, which is equal to 1.1667×10^{-3} kWh/kg.℃. d_{w} stands for the density of water, which is equal to 1000 kg/m^3. $T_{\mathrm{em,in}}(t)$ is the initial temperature of water. $T_{\mathrm{em,min}}$ and$T_{\mathrm{em,max}}$ represent the minimum and maximum acceptable temperature of water, respectively. $V_{\mathrm{w},i}(t)$ is the volume of water supplied to User$_{\mathrm{ct},i}$ at t.

2) Model of User$_{e}$

The optimization target of User$_{\mathrm{e},j}$ is to minimize the operation cost, which consists of the cost for total energy consumption and the economic compensation.

$$F_{\mathrm{e}j}=\min(EC_{e,j}-E_{\mathrm{e}j}) \tag{9}$$

$$EC_{\mathrm{e}j}=\sum\nolimits_{t=1}^{T}P_{\mathrm{e}j}(t)\cdot p_{\mathrm{e}}(t) \tag{10}$$

$$E_{\mathrm{e}j}=\sum\nolimits_{t=T_{\mathrm{s}}}^{T_{\mathrm{e}}}[P_{\mathrm{cur},j}(t)-P_{\mathrm{e}j}(t)]\cdot p_{\mathrm{be}}(t) \tag{11}$$

$$P_{\mathrm{e}j}(t)=P_{\mathrm{cur},j}(t)-\Delta P_{\mathrm{tld},j}(t)-\Delta P_{\mathrm{rld},j}(t) \tag{12}$$

where $F_{\mathrm{e},j}$represents the operation cost of User$_{\mathrm{e},j}$. $EC_{\mathrm{e},j}$ is the electricity cost and $E_{\mathrm{e},j}$ is the economic compensation; $P_{\mathrm{e},j}(t)$ is the electricity consumption of User$_{\mathrm{e},j}$ at t; $p_{\mathrm{e}}(t)$ is the electricity price; $P_{\mathrm{cur},j}(t)$ denotes the electricity consumption in current operation mode at t; The change of electrical load at t is comprised of load transferred $\Delta P_{\mathrm{tld},j}(t)$ and load reduced $\Delta P_{\mathrm{rld},j}(t)$; and $p_{\mathrm{be}}(t)$ is the compensation price for electricity.

Eqs.(13) and (14) are the expressions of the electrical transferable load and the electrical reduced load. Notably, the negative value of $\Delta P_{\mathrm{tld},j}(t)$ indicates that the load is shifted to

t and load at t is increased, otherwise the load at t is reduced.

$$\begin{cases} \sum_{t=1}^{T} \Delta P_{\text{tld}}(t) = 0 \\ |\Delta P_{\text{tld}}(t)| \le P_{\text{tld,max}} \end{cases} \tag{13}$$

$$\begin{cases} \Delta P_{\text{rld}}(t) \in [P_{\text{rld,min}}, P_{\text{rld,max}}] \\ \sum_{t=1}^{T} \Delta P_{\text{rld}}(t) \le P_{\text{rld,max}} \end{cases} \tag{14}$$

where $P_{\text{tld,max}}$ is the maximum transferable power. $P_{\text{rld,min}}$ and $P_{\text{rld,max}}$ represent the minimum and maximum reduced load, respectively. $P_{\text{rld,max}}$ is the maximum reduced electrical load.

3) Model of Operator

The objective function of the multi-energy station (operator) is to maximize net income, which includes the energy income, the economic compensation and cost for purchasing energy.

$$F_{\text{o}} = \max(HI_{\text{o}} + CI_{\text{o}} + E_{\text{o}} - BC_{\text{o}}) \tag{15}$$

$$E_{\text{o}} = \sum_{t=T_s}^{T_e} \Delta P_{\text{o}}(t) \cdot p_{\text{bo}}(t) \tag{16}$$

$$BC_{\text{o}} = \sum_{t=1}^{T} [P_{\text{grid}}(t) \cdot p_{\text{buy}}(t) + V_{\text{gas}}(t).p_{\text{n}}(t)] \tag{17}$$

where objective function F_{o} includes thermal energy income HI_{o}, cooling energy income CI_{o}, compensation income E_{o} and cost for purchasing electricity and gas BC_{o}. $\Delta P_{\text{o}}(t)$ represents the power of operator that participated in AS. $p_{\text{bo}}(t)$ is the compensation price for operator. $p_{\text{buy}}(t)$ is the price for buying electricity $P_{\text{grid}}(t)$ from the power grid at t, and $p_{\text{n}}(t)$ is that for purchasing natural gas from gas station at t. $V_{\text{gas}}(t)$ is the volume of purchased natural gas.

According to Fig. 3, the electricity supply is relied on gas turbine and the power grid. Cooling energy is generated by lithium bromide unit (LBU) and centrifuge. Thermal energy is produced by lithium bromide unit, boiler and heat pump. The model of gas turbine is expressed by Eqs.(18)-(20).

$$P_{\text{ge}}(t) = \eta_{\text{ge,e}} \cdot V_{\text{ge}}(t) \cdot \lambda_{\text{gas}} \tag{18}$$

$$H_{\text{ge}}(t) = \eta_{\text{ge,h}} \cdot V_{\text{ge}}(t) \cdot \lambda_{\text{gas}} \tag{19}$$

$$P_{\text{ge}}(t) \in [P_{\text{ge,min}}, P_{\text{ge,max}}] \tag{20}$$

where $P_{\text{ge}}(t)$ and $H_{\text{ge}}(t)$ represent the output electricity and the waste thermal power at t. $\eta_{\text{ge,e}}$ and $\eta_{\text{ge,h}}$ are the efficiencies for electricity and thermal energy generation, respectively. $V_{\text{ge}}(t)$ is the consumed volume of natural gas in gas turbine. λ_{gas} is the calorific value of natural gas. $P_{\text{ge,min}}$ and $P_{\text{ge,max}}$ represent the minimum and maximum output power.

The model of LBU is given in Eqs.(21)-(23).

$$H_{\text{li}}(t) = s_{\text{li,h}}(t) \cdot c_{\text{li,h}} \cdot H_{\text{ge}}(t) \tag{21}$$

$$C_{\text{li}}(t) = s_{\text{li,c}}(t) \cdot c_{\text{li,c}} \cdot H_{\text{ge}}(t) \tag{22}$$

$$\{C_{\text{li}}(t), H_{\text{li}}(t)\} \in [P_{\text{li,min}}, P_{\text{li,max}}] \tag{23}$$

where $H_{\text{li}}(t)$ and $C_{\text{li}}(t)$ are the generated thermal power and cooling power of LBU at t. $s_{\text{li,h}}(t)$ and $s_{\text{li,c}}(t)$ are binary variables and respectively represent the heating state and cooling state of LBU, which cannot coexist. $c_{\text{li,h}}$ and $c_{\text{li,c}}$ are respectively the heating coefficient and the cooling coefficient of LBU. $P_{\text{li,min}}$ and $P_{\text{li,max}}$ are the minimum and maximum power of LBU, respectively.

The model of heaters (heat pump/boiler) is obtained by

$$H_{\text{h}}(t) = c_{\text{h}} \cdot V_{\text{h}}(t) \cdot \lambda_{\text{gas}} \tag{24}$$

$$H_{\text{h}}(t) \in [H_{\text{h,min}}, H_{\text{h,max}}] \tag{25}$$

where $H_{\text{h}}(t)$ is the heating power of heaters. c_{h} is the heating coefficient. $H_{\text{h,min}}$ and $H_{\text{h,max}}$ denote the minimum and maximum output thermal energy of heaters. $V_{\text{h}}(t)$ is the consumed volume of natural gas in heaters.

The model of centrifuge is

$$C_{\text{cf}}(t) = c_{\text{cf}} \cdot P_{\text{cf}}(t) \tag{26}$$

$$C_{\text{cf}}(t) \in [C_{\text{cf,min}}, C_{\text{cf,max}}] \tag{27}$$

where $C_{\text{cf}}(t)$ is the output cooling power of centrifuge at t. c_{cf} is its cooling coefficient. $P_{\text{cf}}(t)$ is electricity consumption of centrifuge at t. $C_{\text{cf,min}}$ and $C_{\text{cf,max}}$ are the minimum and maximum produced cooling power.

The model of energy storage system is

$$S_{\text{ess}}(t) = \gamma S_{\text{ess}}(t\text{-}1) + \eta_{\text{ch}} \cdot s_{\text{ch}}(t) \cdot P_{\text{ch}}(t\text{-}1) - s_{\text{dis}}(t)\frac{P_{\text{dis}}(t\text{-}1)}{\eta_{\text{dis}}} \tag{28}$$

$$\{P_{\text{ch}}(t), P_{\text{dis}}(t)\} \in [0, P_{\text{ess,max}}] \tag{29}$$

$$S_{\text{ess}}(t) \in [S_{\text{ess,min}}, S_{\text{ess,max}}] \tag{30}$$

$$S_{\text{ess}}(0) = S_{\text{ess}}(T) \tag{31}$$

where $S_{\text{ess}}(t)$ stands for the storage capacity of energy storage system (ESS). γ is its loss rate. η_{ch} and η_{dis} are the charging /discharging efficiencies. $P_{\text{ch}}(t\text{-}1)$ and $P_{\text{dis}}(t\text{-}1)$ represent the charging and discharging power at moment (t-1). $P_{\text{ess,max}}$ represents the maximum charging/discharging power. $S_{\text{ess,min}}$ and $S_{\text{ess,max}}$ are the minimum and maximum capacities of ESS, respectively. $s_{\text{ch}}(t)$ and $s_{\text{dis}}(t)$ are binary variables, which respectively denote the charging state and the discharging state of ESS that cannot coexist.

The electricity, cooling energy and thermal energy are consistent with the energy conservation principle. Due to the paper limit, the balance constraints of them are omitted.

B. Game among Energy Entities

In the designed operation mode, users prone to minimize energy cost and the multi-energy station tends to maximize the energy income. Clearly, there is a confliction among them, which can be regarded as a typical non-cooperative game. With Stackelberg game theory, the game model is shown in Fig. 6.

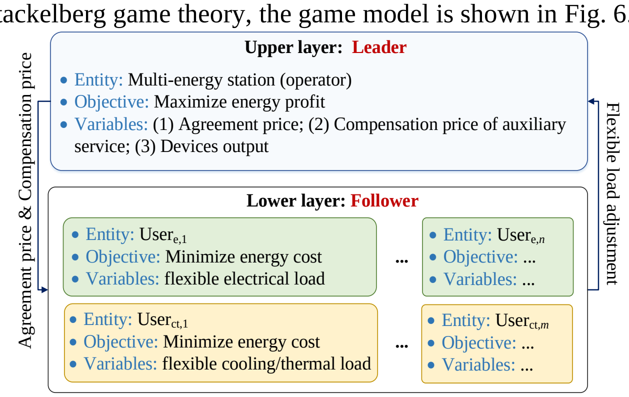

Fig. 6. Game among operator and users.

Optimization of the game among these energy entities is a two-layer dynamic circular process, in which the multi-energy station (operator) is leader, and users are followers. In the upper layer, the operator sends the incentives of agreement price and compensation price to users based on the objective to maximize its energy profit. Then, users in the lower layer report their load profiles to the operator based on their day-ahead energy consumption plan to minimize their own operation cost. After summarizing the load profiles of users, the operator resets the compensation price and agreement price accordingly and sends the price incentives again. The steps repeat until both operator and users cannot achieve better economic benefits by changing energy decisions alone. This state is called game equilibrium.

To balance the game among the operator and multiple users, the determination of the agreement price and compensation prices are of great importance. One of the basic principles to determine the electricity agreement price is that the energy cost of $\mathrm{User_e}$ with agreement price is lower than that in the current operation mode.

$$\sum_{t=1}^{T}\sum_{j=1}^{m} P_{\mathrm{e},j}(t)\cdot p_{\mathrm{e}}(t) \le \mu \cdot EC_{\mathrm{cur}} \tag{32}$$

$$\sum_{t=1}^{T}\frac{p_{\mathrm{e}}(t)}{T} \le p_{\mathrm{e,av}} \tag{33}$$

$$p_{\mathrm{e}}(t) \in [p_{\mathrm{e,min}}, p_{\mathrm{e,max}}] \tag{34}$$

where EC_{cur} is the electricity cost of $\mathrm{User_e}$ in current operation mode, and μ is the reduction coefficient. $p_{\mathrm{e,av}}$ is the upper limit of the average electricity price. $p_{\mathrm{e,min}}$ and $p_{\mathrm{e,max}}$ are the minimum and maximum electricity price at each moment.

The compensation price is a crucial incentive to motivate users to actively respond to the AS demand. The way to pay it to users follows the principals:

$$\frac{\sum_{t=T_{\mathrm{s}}}^{T_{\mathrm{e}}} p_{\mathrm{b}}(t)}{T_{\mathrm{e}}-T_{\mathrm{s}}+1} \in [p_{\mathrm{b,lo}}, p_{\mathrm{b,up}}] \tag{35}$$

$$p_{\mathrm{b}}(t) \in [p_{\mathrm{b,min}}, p_{\mathrm{b,max}}] \tag{36}$$

where $p_{\mathrm{b,lo}}$ and $p_{\mathrm{b,up}}$ denote the lower and upper limits of the average compensation price; $p_{\mathrm{b,min}}$ and $p_{\mathrm{b,max}}$ are the minimum and maximum values of the compensation price for each moment; and $p_{\mathrm{b}}(t)$ refers to the compensation prices for adjusting flexible loads.

C. Model Solving

The game among multiple entities is described as a two-layer optimization problem (as given in Section III.B). The two-layer optimization model can be converted to a single-layer model by using the Karush-Kuhn-Tucker (KKT) condition to transform the lower layer to the constraints of upper layer [22]. Then, the optimal solution or the equilibrium point of the game is found by using GAMS software [23].

Since the energy price $\{p_{\mathrm{h}}(t), p_{\mathrm{c}}(t)\}$ and compensation price $p_{\mathrm{b}}(t)$ for thermal and cooling energy are the same, the model of $\mathrm{User}_{\mathrm{ct},i}$ (Eqs.(1)-(8)) can be simplified by cutting down the number of control variables:

$$\begin{cases} \min[\sum_{t=1}^{T} Q_{\mathrm{ct},i}(t)\cdot p_{\mathrm{pur}}(t) - \sum_{t=T_{\mathrm{s}}}^{T_{\mathrm{e}}} \Delta Q_{\mathrm{ct},i}(t)\cdot p_{\mathrm{b}}(t) \\ \mathrm{s.t.}\begin{cases} \Delta Q_{\mathrm{ct},i}(t) - Q_{\mathrm{cur},i}(t) + Q_{\mathrm{ct},i}(t) = 0 \\ Q_{\mathrm{ct},i}(t) - Q_{\mathrm{max},i} \le 0,\ Q_{\mathrm{min},i} - Q_{\mathrm{ct},i}(t) \le 0 \end{cases} \end{cases} \tag{37}$$

where $Q_{\mathrm{ct},i}(t)$ is the thermal/cooling power consumption at t; $p_{\mathrm{pur}}(t)$ denotes purchasing price for thermal/cooling energy. Clearly, there are two control variables ($Q_{\mathrm{ct},i}(t)$ and $\Delta Q_{\mathrm{ct},i}(t)$), one equation constraint and two inequality constraints.

The constraints based on KKT condition of $\mathrm{User}_{\mathrm{ct},i}$ is

$$\begin{cases} \sum_{t=1}^{T} p_{\mathrm{pur}}(t) + L(t) + M_1(t) - M_2(t) = 0 \\ -\sum_{t=T_{\mathrm{s}}}^{T_{\mathrm{e}}} p_{\mathrm{b}}(t) + L(t) = 0, \forall t \in [T_{\mathrm{s}}, T_{\mathrm{e}}] \\ L(t) = 0, \forall t \notin [T_{\mathrm{s}}, T_{\mathrm{e}}] \\ \Delta Q_{\mathrm{ct},i}(t) - Q_{\mathrm{cur},i}(t) + Q_{\mathrm{ct},i}(t) = 0 \\ f_k(t) \le 0, k = 1,2 \\ M_k(t) \ge 0, k = 1,2 \\ M_k(t)\cdot f_k(t) = 0, k = 1,2 \end{cases} \tag{38}$$

where $f_k(t)$ denotes the k^{th} inequality constraints; $L(t)$ is the Lagrange multiplier for equality constraint, and $M_k(t)$={$M_1(t)$, $M_2(t)$} are Lagrange multipliers for inequality constraints.

The standardized expression of the model of $\mathrm{User}_{\mathrm{e},j}$ is obtained by Eq.(39), and it includes three control variables ($P_{\mathrm{e},j}(t)$, $\Delta P_{\mathrm{tld},j}(t)$ and $\Delta P_{\mathrm{rld},j}(t)$), two equality constraints and five inequality constraints.

$$\begin{cases} \min[\sum_{t=1}^{T} P_{\mathrm{e},j}(t)\cdot p_{\mathrm{e}}(t) - \sum_{t=T_{\mathrm{s}}}^{T_{\mathrm{e}}} [P_{\mathrm{cur},j} - P_{\mathrm{e},j}(t)]\cdot p_{\mathrm{be}}(t) \\ \mathrm{s.t.}\begin{cases} P_{\mathrm{e},j}(t) - P_{\mathrm{cur},j}(t) + \Delta P_{\mathrm{tld},j}(t) + \Delta P_{\mathrm{rld},j}(t) = 0 \\ \sum_{t=1}^{T} \Delta P_{\mathrm{tld}}(t) = 0 \\ \Delta P_{\mathrm{tld}}(t) - \mathrm{P}_{\mathrm{tld,max}} \le 0, -\mathrm{P}_{\mathrm{tld,max}} - \Delta P_{\mathrm{tld}}(t) \le 0 \\ \Delta P_{\mathrm{rld}}(t) - \mathrm{P}_{\mathrm{rld,max}} \le 0,\ P_{\mathrm{rld,min}} - \Delta P_{\mathrm{rld}}(t) \le 0 \\ \sum_{t=1}^{T} \Delta P_{\mathrm{rld}}(t) - P_{\mathrm{rld,max}} \le 0 \end{cases} \end{cases} \tag{39}$$

Accordingly, the constraints based on KKT condition of $\mathrm{User}_{\mathrm{e},j}$ is

$$\begin{cases} \sum_{t=1}^{T} p_{\mathrm{e}}(t) + \sum_{t=T_{\mathrm{s}}}^{T_{\mathrm{e}}} p_{\mathrm{be}}(t) + L_1(t) = 0, \forall t \in [T_{\mathrm{s}}, T_{\mathrm{e}}] \\ \sum_{t=1}^{T} p_{\mathrm{e}}(t) + L_1(t) = 0, \forall t \notin [T_{\mathrm{s}}, T] \\ L_1(t) + \sum_{t=1}^{T} L_2(t) + M_1(t) - M_2(t) = 0 \\ L_1(t) + M_3(t) - M_4(t) + \sum_{t=1}^{T} M_5(t) = 0 \\ g_r(x) = 0, r = 1,2 \\ f_k(x) \le 0, k = 1,2,...,5 \\ M_k(t) \ge 0, k = 1,2,...,5 \\ M_k(t)\cdot f_k(x) = 0, k = 1,2,...,5 \end{cases} \tag{40}$$

where $g_r(x)$ refers to the r^{th} equality constraints. $L_r(t) = \{L_1(t), L_2(t)\}$ are the Lagrange multipliers for equality constraints; $M_k(t)$ ={ $M_1(t)$,…, $M_5(t)$ } are the Lagrange multipliers for inequality constraints.

D. Overview Diagram

An overview diagram of the proposed operation approach is provided in Fig. 7. Notably, the dispatch period is one day, with the time interval of 15 minute, i.e., T=96. The load profiles of users without flexible load adjustment in MEMG is predicted by a combined load forecasting method in the previous day [24].

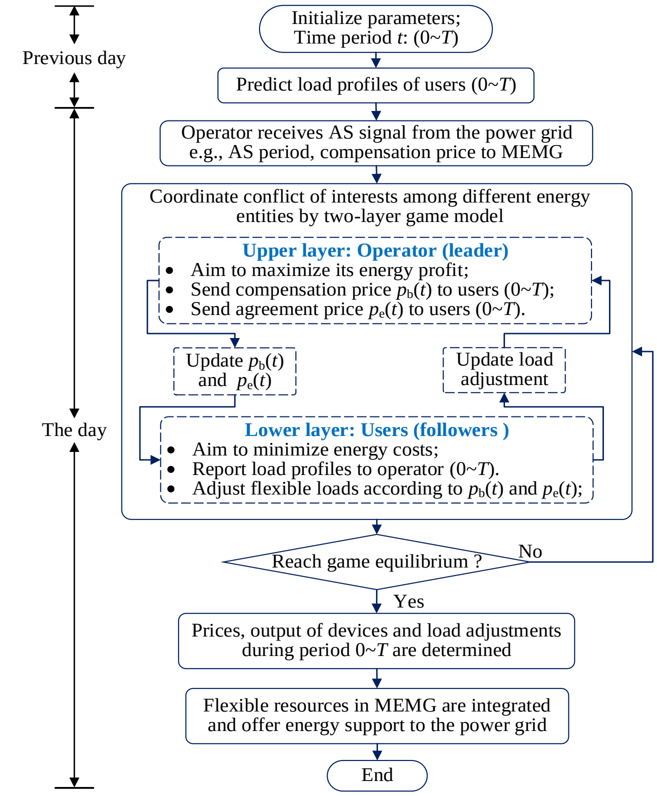

Fig. 7. An overview diagram of the proposed operation strategy.

IV. Validation and Analysis

A. Data and Parameters

The data used in this paper is collected from the practical MEMG project in July, 2021. The cooling and thermal loads of User_{ct} and the electricity consumption of User_{e} are respectively shown in Fig. 8 (a)-(c).

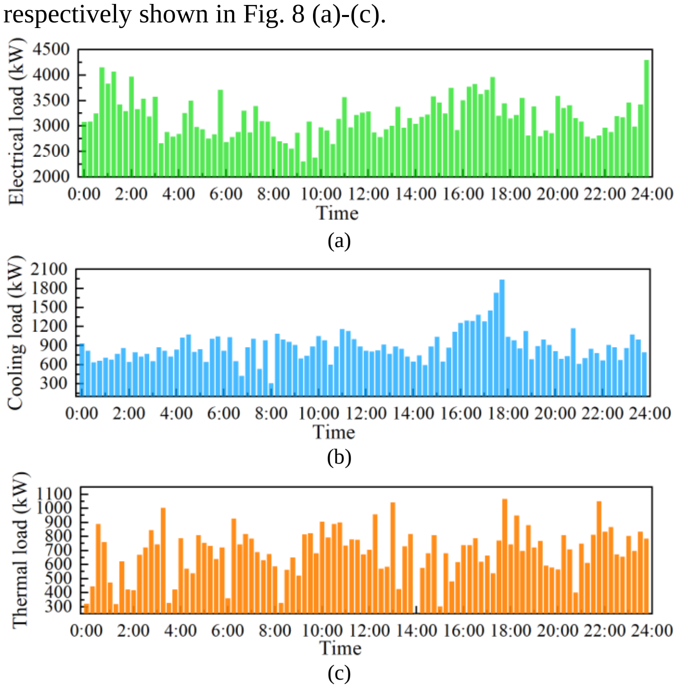

Fig. 8 Load profiles in one day. (a) Electrical load of User_{e}; (b) Cooling load of User_{ct}; (c) Thermal load of User_{ct}.

The operation parameters of the MEMG are given in Table II. The electricity price of the power grid is given in Table III, and agreement/ compensation prices are shown in Table IV. The parameters of flexible electrical load and thermal/cooling load are respectively presented in Table V and Table VI. Table VII displays the device parameters.

TABLE II
Operation Parameters of the MEMG

Content	Value	Content	Value
Dispatch period	One day	AS period	16:00-18:00
Dispatch interval	15 minutes	Gas price	3.28 Yuan/m^3
Cooling energy price	0.5 Yuan/kWh	Thermal energy price	0.5 Yuan/kWh

TABLE III
Electricity Price of Power Grid

Period	19:00-22:00	8:00-11:00 15:00-19:00	7:00-8:00 11:00-15:00 22:00-23:00	23:00-7:00
Price (Yuan/kWh)	0.88405	0.78405	0.63405	0.43405

TABLE IV
Parameters of Agreement Price and Compensation Prices

Prices	Parameters	Value (Yuan/kWh)
Electricity agreement price	Upper limit of average price $p_{\text{e,av}}$	0.7
	Reduction coefficient μ	0.95
	Minimum price $p_{\text{e,min}}$	0.4
	Maximum price $p_{\text{e,max}}$	1.0
Compensation price for operator/MEMG	Price at t (during AS period) $p_{\text{bo}}(t)$	1.2
	Price at t (not in AS period) $p_{\text{bo}}(t)$	0
Compensation price for User_{e}	Lower limit of average price $p_{\text{b,lo}}$	0.9
	Upper limit of average price $p_{\text{b,up}}$	1.1
	Minimum price $p_{\text{b,min}}$	0.8
	Maximum price $p_{\text{b,max}}$	1.2
Compensation price for User_{ct}	Lower limit of average price $p_{\text{b,lo}}$	0.25
	Upper limit of average price $p_{\text{b,up}}$	0.3
	Minimum price $p_{\text{b,min}}$	0.24
	Maximum price $p_{\text{b,max}}$	0.4

TABLE V
Parameters of Flexible Electrical Load

Load type	Parameters	Value
Transferable load	Maximum transferred power	∓300 kW
Reduced load	Minimum reduced power	100 kW
	Maximum reduced power	200 kW
	Maximum reduced energy	7624 kWh

TABLE VI
Parameters of Thermal/Cooling Loads

Load type	Temperature of supply water	Maximum temperature of return water	Minimum temperature of return water
Thermal load	80 °C	56°C	54°C
Cooling load	6 °C	14 °C	12 °C

TABLE VII
Parameters of Equipment in MEMG

Equipment	Parameters	Value
Gas turbine	Rated power	2 MW
	Electricity efficiency $\eta_{\text{ge,e}}$	0.45
	Thermal efficiency $\eta_{\text{ge,h}}$	0.35
LBU	Rated power	2.326 MW
	Cooling coefficient $c_{\text{li,c}}$	1.2
	Heating coefficient $c_{\text{li,h}}$	0.8
Boiler	Rated power	1.29 MW
	Thermal coefficient c_{h}	0.95
Heat pump	Rated power	1632 kWh
	Thermal coefficient c_{h}	1.2
Centrifuge	Rated power	9.829 MW
	Cooling coefficient c_{cf}	3.0
Thermal ESS	Maximum capacity $S_{\text{ess,max}}$	1680 kWh
	Minimum capacity $S_{\text{ess,min}}$	200 kWh
	Maximum charging/discharging power $P_{\text{ess,max}}$	700/700 kW
	Charging/discharging efficiency $\eta_{\text{ch/dis}}$	0.96/0.96
	Loss rate γ	0.98

B. *Validation of the Strategy*

1) *Energy dispatching*

When the proposed operation strategy is applied, the supply and demand of electricity, cooling energy and thermal energy in the MEMG are respectively shown in Fig. 9 to Fig. 11.

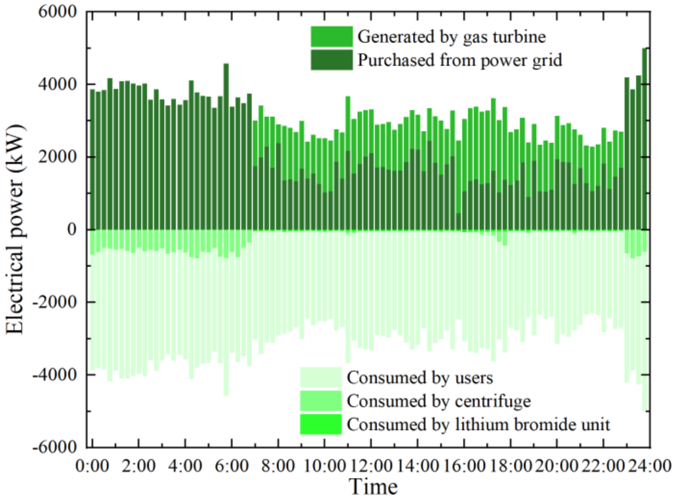

Fig. 9 Supply and demand of electricity in the MEMG.

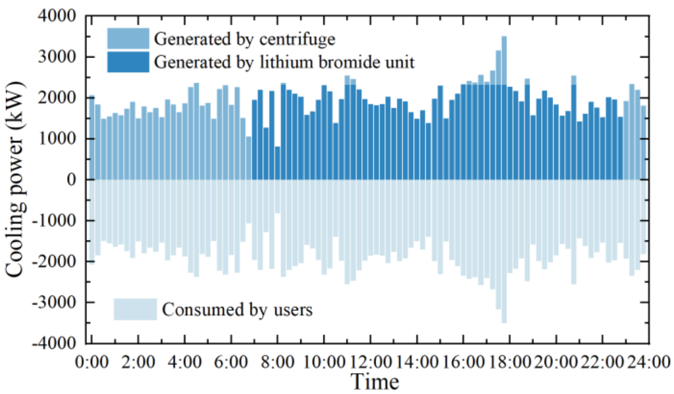

Fig. 10 Supply and demand of cooling energy in the MEMG.

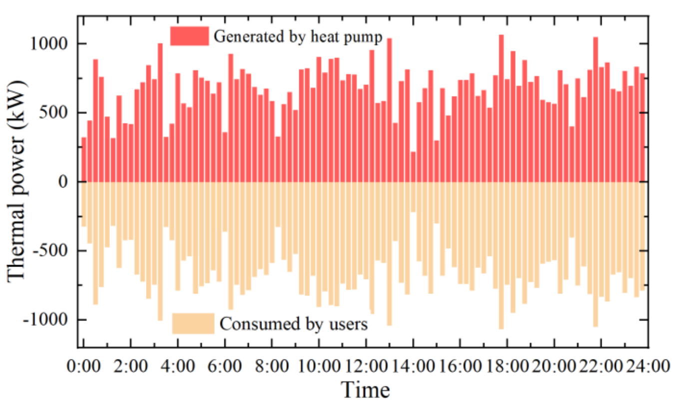

Fig. 11 Supply and demand of thermal energy in the MEMG.

In Fig. 9, the gas turbine is not running and all the electricity demand of the MEMG is provided by the power grid during 23:00-7:00, since the electricity price of power grid is the lowest during this period. For the rest of the time, particularly in the peak-saving AS period (16:00-18:00), the gas turbine works at full capacity to respond to the AS signal, reducing the electricity cost and increasing the compensation for joining AS.

In Fig. 10, during 23:00-7:00, the centrifuge is used in priority due to its higher cooling coefficient compared with LBU. For the rest of the time, most of the cooling energy is offered by LBU because of the waste heat recovery of gas turbine.

As in Fig. 11, the thermal load is relatively small in summer compared with electrical and cooling energy consumptions, and all the thermal energy is provided by heat pump due to its higher thermal coefficient comparing with boiler.

2) *Prices determination*

Based on price constraints and the two-layer game model, the electricity agreement price and the compensation prices are determined, as displayed in Fig. 12 and Fig. 13, respectively.

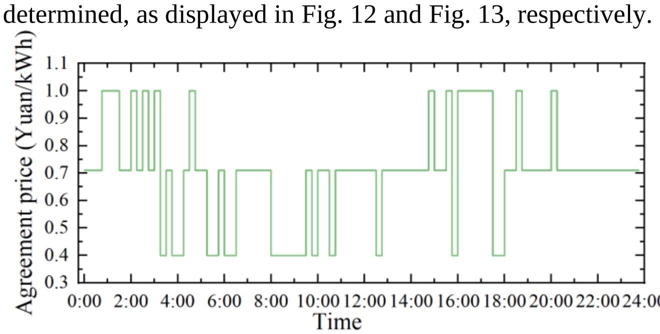

Fig. 12 Electricity agreement price for User$_e$.

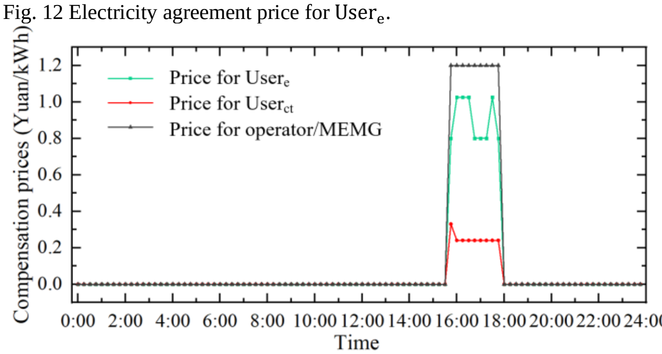

Fig. 13 Compensation prices for operator/MEMG and users.

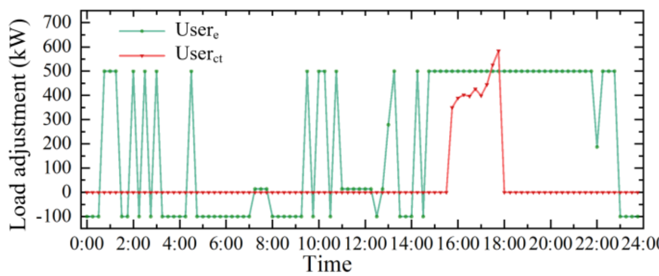

Fig. 14 Load adjustment of users.

The load adjustment of users that responds to the price incentives is shown in Fig. 14. When power change greater than 0, it indicates that the power is increasing; otherwise, it is reducing. The agreement price, compensation prices and flexible loads adjustment are interactional, as they are control variables of the two-layer game model. For instance, the compensation price for User$_{ct}$ is higher during 16:00-16:15 comparing with the rest of the AS period. The reason lies in the fact that User$_{ct}$ have the least ability to respond to the peak-shaving demand at this time. Accordingly, the compensation price is increased to driven User$_{ct}$ to adjust load.

C. *Comparative Cases*

To verify the feasibility of the proposed operation strategy of MEMG, four cases are set up, as shown in Table VIII. Notably, Case 1 indicates the current operation mode of the MEMG, which can be regarded as a benchmark for other cases. Case 4 is with the proposed operation approach. The effectiveness of the proposed method can be derived via the comparative analysis of the four cases.

TABLE VIII
FOUR CASES FOR COMPARATIVE ANALYSIS

Cases	Settings
Case 1	Without operator, AS and IDR
Case 2	With operator and AS; without IDR
Case 3	With operator, AS, IDR and fixed agreement/compensation prices
Case 4	With operator, AS, IDR and prices based on game model

1) *Economic benefits*

The daily operation cost of $\mathrm{User_{ct}}$ and $\mathrm{User_e}$ in the four cases are shown in Fig. 15 and Fig. 16, respectively. The net income of operator in the four cases are given in Fig. 17. Case 1 is used as the benchmark to calculate change ratio of each case.

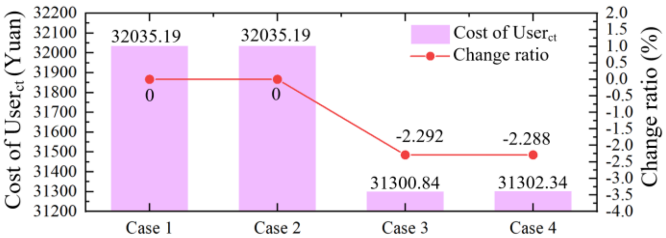

Fig. 15 Daily operation costs and change ratios of $\mathrm{User_{ct}}$ in the four cases.

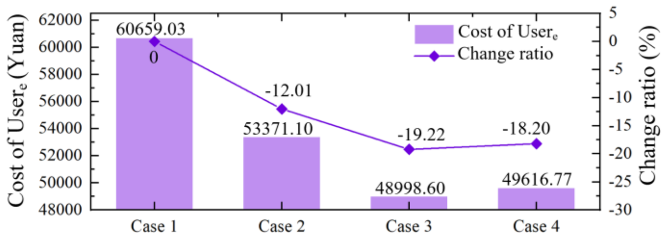

Fig. 16 Daily operation costs and change ratios of $\mathrm{User_e}$ in the four cases.

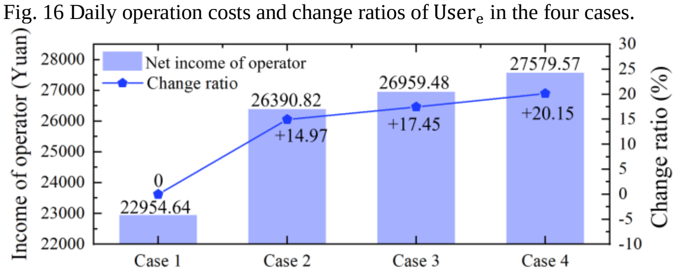

Fig. 17 Net incomes and change ratios of operator in the four cases.

Comparing Case 2 with Case 1, the daily operation cost of $\mathrm{User_e}$ is reduced by 12.01% and the daily net income of the operator is increased by 14.97%. It reflects that when the multi-energy station works as the operator of the MEMG and trade electricity directly with $\mathrm{User_e}$, both the operator and users gain more economic benefits. When comparing Case 3 with Case 2, an obvious reduction of the daily operation cost of users and fast growth in daily revenue of the operator can be observed, it is mainly resulted from the employment of IDR in Case 3. The comparison of Case4 and Case 3 shows that the proposed operation strategy can coordinate the conflicting interests among different energy entities and provide an opportunity for the operator to gain more profit.

2) *Energy integration*

Compared with the benchmark (Case 1), the power change of MEMG in other cases during the AS period can reflect the energy integration capability of MEMG by operator, i.e., larger power change indicates that more flexible resources in the MEMG are integrated to participate in peak-shaving AS.

The power change of MEMG during the AS period (16:00-18:00) in the four cases are shown in Fig. 18. Clearly, compared with Case 2, MEMG shows greater peak-shaving ability in Case 3 and Case 4 when IDR is employed. As given in Table IX, with the proposed strategy, the greatest energy integration ability of MEMG in Case 4 leads to the highest compensation income and net income of the operator.

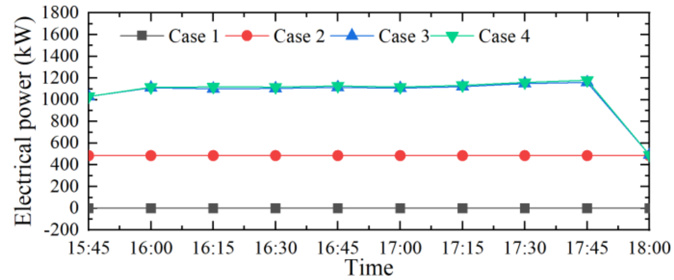

Fig. 18 Power change of MEMG during AS period in the four cases.

TABLE IX
DETAILED INCOMES AND COSTS OF THE OPERATOR

Case	Energy income (Yuan)	Compen. income (Yuan)	Compen. to users (Yuan)	Electricity cost (Yuan)	Gas cost (Yuan)	Net income (Yuan)
Case 1	92694.2	0	0	0	69739.4	22954.6
Case 2	85406.2	1308.6	0	35822.4	24501.6	26390.8
Case 3	80299.4	2873.7	1190.6	30521.4	24501.6	26959.5
Case 4	82174.8	3028.7	1254.8	31867.5	24501.6	27579.6

Compen.="Compensation"

3) *User satisfaction*

To participate in AS market, IDR is applied and flexible loads in MEMG are adjusted according to the AS demand. However, it is realized via users changing their energy consumption behaviors, which would affect their comfort and reduce their satisfaction. Due to the larger proportion and higher flexibility of electrical load in MEMG compared with cooling and thermal load, the user satisfaction analysis of $\mathrm{User_e}$ is representative. In Fig. 19, the difference of the load curves of $\mathrm{User_e}$ in the four cases can be visually observed.

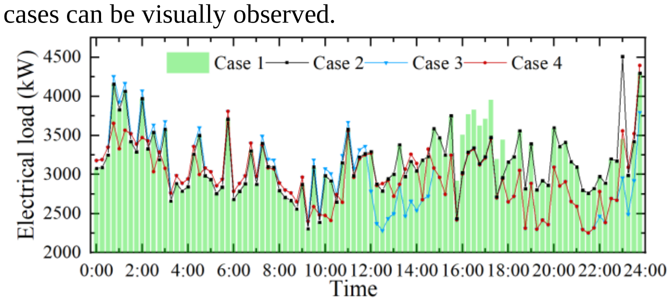

Fig. 19 Load curves of $\mathrm{User_e}$ in the four cases.

To quantify the load changes of users, an evaluation index *USI* is proposed in Eq.(41).

$$\begin{cases} USI = \dfrac{P_{\mathrm{av}} - \Delta P_{\mathrm{av}}}{P_{\mathrm{av}}} \times 100\% \\ \Delta P_{\mathrm{av}} = \dfrac{\sum_{t=1}^{T} |\Delta P(t)|}{T} \\ P_{\mathrm{av}} = \dfrac{\sum_{t=1}^{T} |P(t)|}{T} \end{cases} \tag{41}$$

where $P(t)$ is load power at t of the benchmark (Case 1) and $\Delta P(t)$ denotes power change at t compared to the benchmark.

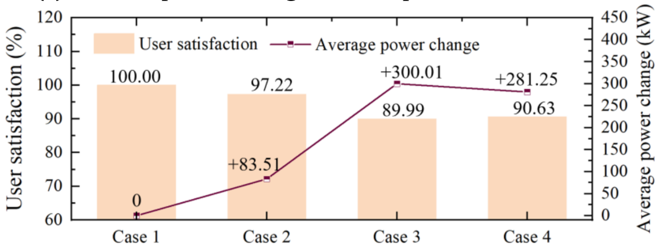

Fig. 20 User satisfaction and average power change in the four cases.

The value of *USI* and average power changes in the four cases are shown in Fig. 20. IDR is applied in both Case 3 and Case 4, but the *USI* of Case 4 is higher than that of Case 3. Obviously, consumption behavior of users is maintained better with the proposed operation strategy compared with Case 3.

V. Conclusions and Future Works

A practical case of MEMG participating AS is investigated in this paper. An optimal operation strategy for MEMG is proposed to handle relevant critical issues, e.g., coordination of conflicting interest among multiple energy entities, adjustment of flexible loads in various forms and integration multiple flexible resources in energy supply and demand sides. The following conclusions are drawn according to the results: 1) with the employment of IDR, the proposed strategy is a win-win mechanisms for both the operator and the users, increasing the overall net income of operator and reducing the energy consumption cost of users; 2) the proposed strategy coordinates conflicting interests of multiple energy entities via two-layer game model and help MEMG gain more profit via participating AS; 3) user satisfaction is maintained by the proposed strategy through rationally adjusting energy consumption.

To further improve the proposed operation methodology, there are several research directions for future works: 1) establish more precise model of equipment and take specific network parameters and practical constraints into account when modeling; 2) investigate on solution techniques with higher convergency speed and computational accuracy; 3) carry out robust optimization of MEMG by considering uncertainty of energy supply and demand sides; and 4) Extend the operation strategy to larger microgrid.

References

[1] J. Zeng, Q. Wang, J. Liu, *et al.*, "A potential game approach to distributed operational optimization for microgrid energy management with renewable energy and demand response," *IEEE Trans. Ind. Electron.*, vol. 66, no. 6, pp. 4479–4489, 2019.

[2] M. H. Cintuglu, H. Martin, and O. A. Mohammed, "Real-time implementation of multiagent-based game theory reverse auction model for microgrid market operation," *IEEE Trans. Smart Grid*, vol. 6, no. 2, pp. 1064–1072, 2017.

[3] J. Liu, X. Chen, H. Liu, *et al.*, "Optimal bidding strategy of load aggregators for the auxiliary service market of peak shaving and valley filling," in *Proceedings-2021 IEEE International Conference on Energy Internet, ICEI*, 2021, pp. 205–210.

[4] F. Arasteh and G. H. Riahy, "MPC-based approach for online demand side and storage system management in market based wind integrated power systems," *Int. J. Electr. Power Energy Syst.*, vol. 106, pp. 124–137, 2019.

[5] L. Chen, J. Wu, H. Zhang, *et al.*, "Robust optimization based coordinated scheduling strategy for integrated demand response in micro energy grid (in Chinese)," *Autom. Electr. Power Syst.*, vol. 21, pp. 159–169, 2021.

[6] Y. Zhou, J. Wu, G. Song, *et al.*, "Framework design and optimal bidding strategy for ancillary service provision from a peer-to-peer energy trading community," *Appl. Energy*, vol. 278, p. 115671, 2020.

[7] D. Kotur and Ž. Đurišić, "Optimal spatial and temporal demand side management in a power system comprising renewable energy sources," *Renew. Energy*, vol. 108, pp. 533–547, 2017.

[8] J. Hu, X. Liu, M. Shahidehpour, *et al.*, "Optimal operation of energy hubs with large-scale distributed energy resources for distribution network congestion management," *IEEE Trans. Sustain. Energy*, vol. 12, no. 3, pp. 1755–1765, 2021.

[9] P. Li, W. Sheng, Q. Duan, *et al.*, "A Lyapunov optimization-based energy management strategy for energy hub with energy router," *IEEE Trans. Smart Grid*, vol. 11, no. 6, pp. 4860–4870, 2020.

[10] R. B. Myerson, *Game theory: Analysis of conflict*. Harvard University Press, 1997.

[11] Y. Wang, Y. Cao, Y. Li, *et al.*, "Modelling and analysis of a two-level incentive mechanism based peer-to-peer energy sharing community," *Int. J. Electr. Power Energy Syst.*, vol. 133, p. 107202, 2021.

[12] M. Wei, Y. Deng, M. Long, *et al.*, "Transaction model based on Stackelberg game method for balancing supply and demand Sides of multi-Energy microgrid," *Energies*, vol. 15, no. 4, p. 1362, 2022.

[13] Y. Wang, Z. Han, H. V. Poor, *et al.*, "A game-theoretic approach to energy trading in the smart grid," *IEEE Trans. Smart Grid*, vol. 5, no. 3, pp. 1439–1450, 2014.

[14] J. Lee, J. Guo, and M. Zukerman, "Distributed energy trading in microgrids: A game-theoretic model and its equilibrium analysis," *IEEE Trans. Ind. Electron.*, vol. 62, no. 6, pp. 3524–3533, 2015.

[15] A. Chi, "Coalitional game-based cost optimization of energy portfolio in smart grid communities," *IEEE Trans. Smart Grid*, vol. 10, no. 2, pp. 1960–1970, 2019.

[16] R. Zhang, X. Cheng, and L. Yang, "Energy management framework for electric vehicles in the smart grid: A three-party game," *IEEE Commun. Mag.*, vol. 54, no. 12, pp. 93–101, 2016.

[17] C. Li, W. Cai, H. Luo, *et al.*, "Power utilization strategy in smart residential community using non-cooperative game considering customer satisfaction and interaction," *Electr. Power Syst. Res.*, vol. 166, pp. 178–189, 2019.

[18] Y. Long, Y. Li, Y. Wang, *et al.*, "Low-carbon economic dispatch considering integrated demand response and multistep carbon trading for multi-energy microgrid," *Sci. Rep.*, vol. 12, no. 1, pp. 1–13, 2022.

[19] Y. Wang, Y. Ma, F. Song, *et al.*, "Economic and efficient multi-objective operation optimization of integrated energy system considering electro-thermal demand response," *Energy*, vol. 205, p. 118022, 2020.

[20] S. Zheng, Y. Sun, B. Li, *et al.*, "Incentive-based integrated demand response for multiple energy carriers considering behavioral coupling effect of consumers," *IEEE Trans. Smart Grid*, vol. 11, no. 4, pp. 3231–3245, 2020.

[21] Q. Yan, M. Zhang, H. Lin, *et al.*, "Two-stage adjustable robust optimal dispatching model for multi-energy virtual power plant considering multiple uncertainties and carbon trading," *J. Clean. Prod.*, vol. 336, p. 130400, 2022.

[22] A. B. Zemkoho and S. Zhou, "Theoretical and numerical comparison of the Karush-Kuhn-Tucker and value function reformulations in bilevel optimization," *Comput. Optim. Appl.*, vol. 78, no. 2, pp. 625–674, 2021.

[23] "General AlgebraicModeling System (GAMS) Release 25.0.2," 2021. https://www.gams.com

[24] Y. Guo, Y. Li, X. Qiao, *et al.*, "BiLSTM multi-task learning based combined load forecasting considering the loads coupling relationship for multi-energy system," *IEEE Trans. Smart Grid*, vol. 13, no. 5, pp. 3481–3492, 2022.

Yahui Wang was born in Hunan, China, in 1993. She received the B.Sc. degree from the College of Electrical and Information Engineering, Hunan University, Changsha, China, in 2016. Currently, she is taking a successive postgraduate and doctoral program in Hunan University, in Electrical Engineering. Her research interests include the optimization of smart grid, integrated multi-energy systems, and demand-side management.

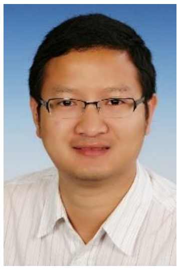

Yong Li was born in Henan, China, in 1982. He received the B.S. and Ph.D. degrees in 2004 and 2011, respectively, from the College of Electrical and Information Engineering, Hunan University, Changsha, China. In 2012, he received the second Ph.D. degree in TU Dortmund University, Dortmund, Germany. Since 2014, he is a Full Professor of electrical engineering with Hunan University. His research interests include power system stability analysis and control, ac/dc energy conversion systems and equipment, analysis and control of power quality, and HVDC and FACTS technologies.

Yijia Cao was born in Hunan, China, in 1969. He received the B.S. from Xi'an Jiaotong University, Xi'an, China, in 1988, and received the M.Sc. and Ph.D. degrees from Huazhong University of Science and Technology, Wuhan, China, in 1991 and 1994, respectively. From 1994 to 2000, he worked as a Visiting Research Fellow and Research Fellow at Liverpool University, Loughborough University, and University of the West England, U.K. Currently, he is the President of Changsha University of Science and Technology, Changsha, China. His research interests include power system stability control and the application of intelligent systems in power systems.

Mohammad Shahidehpour (Life Fellow, IEEE) received the Honorary Doctorate degree in electrical engineering from the Polytechnic University of Bucharest, Romania. He is a University Distinguished Professor with the Illinois Institute of Technology, where he also serves as the Bodine Chair Professor and the Director of the Robert W. Galvin Center for Electricity Innovation. He is a member of the U.S. National Academy of Engineering, and he is also a Fellow of the American Association for the Advancement of Science and the National Academy of Inventors.

Lin Jiang received the B.S and M.S. degrees in electrical engineering from the Huazhong University of Science and Technology, Wuhan, China, in 1992 and 1996, respectively, and the Ph.D. degree in electrical engineering from the University of Liverpool, Liverpool, U.K., in 2001. He is currently a Reader of electrical engineering with the University of Liverpool. His current research interests include control and analysis of power system, smart grid, and renewable energy.

Yilin Long was born in Hunan, China in 1997. She received the B.S. and M.S. degrees from Hunan University, Changsha, China in 2019 and 2022, respectively. She is currently working in State Grid Hunan Power Supply Service Center (Metrology Center). Her research interests include optimized operation and planning of integrated energy system.

Youyue Deng was born in Guangdong, China in 1997. She received the B.S. degree in electrical engineering and its automation from Hunan University, Changsha, China in 2020. She is currently pursuing the M.S. degree in electrical engineering at Hunan University. Her research interests include the optimization and control of smart grid, integrated multi-energy systems, and demand response.

Weiwei Li was born in Hunan, China in 1985. He received the B.S. degree in Construction Environment and Equipment Engineering from Hebei University of Technology in Tangshan, China, in 2007. He has been engaged in the development of integrated energy systems for 15 years, and has rich experience in integrated energy system design, engineering implementation and project operation. He is currently the head of the Integrated Energy Division of ENN Gas Co., Ltd, Changsha, China.